

# Automatic 3-D Modeling of Textured Cultural Heritage Objects

Marco Andreetto, Nicola Brusco, and Guido Maria Cortelazzo

**Abstract**—A widespread use of three-dimensional (3-D) models in cultural heritage application requires low cost equipment and technically simple modeling procedures. In this context, methods for automatic 3-D modeling of textured objects will play a central role. Such methods need fully automatic techniques for 3-D views registration and for the removal of texture artifacts. This paper proposes a contribution in this direction based on image processing approaches. The proposed procedure is very robust and simple. It does not require special equipment or skill in order to make textured 3-D models. The results of this paper, originally conceived to address the costs issues of cultural heritage modeling, can be profitably exploited also in other modeling applications.

**Index Terms**—Automatic modeling, cultural heritage, texture blending, three-dimensional (3-D) registration, wide-baseline matching.

## I. INTRODUCTION

THREE-DIMENSIONAL (3-D) modeling free-form surfaces is well established in some niche applications such as automobile industry, fiction and cartoon movies, special surgery and industrial mechanics, to name a few, where it is customary to model 3-D geometry according to the following pipeline which has range data as input:

- 1) pairwise registration or alignment of the 3-D views;
- 2) global alignment;
- 3) fusion of 3-D data originally captured as clouds of points into a single 3-D surface;
- 4) postprocessing, such as editing of possible surface holes due to minor missing data, or 3-D surface simplification.

In the scientific community the interest for 3-D modeling statues or, in general, cultural heritage's objects such as vases, jewelry, etc., is gaining interest because of its technical challenges; see, for instance, [1]. The modeling difficulties of cultural heritage objects are due to many causes, such as their shape, typically way more articulated than that of mechanical objects; their size, which may not be small; the need to acquire color appearance or reflectance information, whereas in most industrial applications only the geometrical data are of concern; the fact that they cannot be taken into a laboratory but almost always need portable equipment; the prescribed geometrical precision, if physical duplication has to be included among the possible

model's uses or for special investigations, such as the detection of the specific types of chisel marks used by Michelangelo in his sculptures [2], [3].

There is general consensus about the fact that the documentation of heritage's objects should not just concern their geometrical characteristics but also their color, possibly in terms of their reflectance characteristics (typically in terms of estimates of the bi-directional reflectance distribution function (BRDF) [3]–[5]). Because of this, in the case of cultural heritage's objects, the above 3-D modeling pipeline must be extended to include provisions concerning texture acquisition and processing. A very general scheme for the realization of textured 3-D models which essentially couples the standard 3-D geometry construction pipeline concerning the range data with a second pipeline concerning intensity data is presented in [6]. Within the general scheme of [6] many different cost/performance solutions are possible.

Three-dimensional modeling cultural heritage with metrological documentation aims, has recently received a lot of attention from the scientific community. In principle, micrometric precision is easy to reach provided that the instruments and procedures of industrial metrology are employed [2], in practice their application outside laboratory conditions on heritage's objects is a major technical endeavor, not to mention the difficulties related to the in-field acquisition of reflectance or color appearance information. Major efforts in this area were the "Digital Michelangelo Project" [3] and the "Pietà Rondanini Project" [7], both concerning Michelangelo's artworks, the modeling of the relics of the Museum of Quin Shihuang Terra Cotta Warriors and Horses [8] and of the 13 m high Kamakura's Buddha [9]. Among the several other initiatives which took place worldwide [2] we would like to recall the acquisition campaign of the statues of Donatello and Giovanni Pisano jointly performed by the Visual Information Technology Group of the NRC of Ottawa, Canada, and our group [2], [10]–[12] during summer 1997, because it was the first operation of this kind in Italy and because it triggered a number of related initiatives in our country [10], [13]–[17].

Metrological documentation, whether concerning some industrial application or heritage, is only feasible upon adequate financial resources. Therefore, in that context, automatic modeling and low cost acquisition equipment are somewhat secondary with respect to the data's accuracy. However, low costs and operation simplicity are major issues in order to replace the current iconographic material concerning cultural heritage based on photographs with 3-D models, for a better understanding and appreciation of 3-D objects. Indeed it has been long recognized [18] that 3-D objects cannot be adequately

Manuscript received June 25, 2003; revised July 28, 2003. This work was supported by the CNR "Progetto finalizzato Beni Culturali" and by the University of Padova under "Progetto di Ateneo RIA CB 410 Resp. 002064." The associate editor coordinating the review of this manuscript and approving it for publication was Dr. Alessandro Piva.

The authors are with the Department of Information Engineering, University of Padova, 35131 Padova, Italy (e-mail: corte@dei.unipd.it).

Digital Object Identifier 10.1109/TIP.2003.821351

represented by single pictures or collections of pictures, which can only reproduce one viewpoint or a collection of viewpoints, or even by movies, which can reproduce only one visualization trajectory: the one which was followed by the operator during the taking. What characterizes human inspection is the viewer's freedom to choose at any instant his viewing distance and angle in space. The possibility of dynamically visualizing any view of a 3-D object upon users' interaction offered by 3-D models is the representation tool closest to direct inspection. In this context the object's color appearance is essential.

The economic costs implied by a widespread use of 3-D models in cultural heritage are much greater than those for a highly accurate 3-D documentation of a limited selection of masterpieces. In order to appreciate this, as a simple example consider the city museum of Padova, which is an average size museum in Italy with about 1000 statues of various sizes in its art collection and about 5000 objects of various type in its archaeological (pre-Roman and Roman) collection. The total number of museums (of any size) in Italy is 3300. It is considered fair to assume that the Italian museums of average size are about 500 and that the number of items of the city museum of Padova is representative of the average situation. This may give a feeling for the number of heritage's objects one could digitize only in Italy and explains the concern for this issue in some technical literature [11], [19].

The implications of labor costs are more relevant than those of the scanning equipment, since the incidence of the latter decreases with the number of modeled objects, but that of the former doesn't. Labor costs are due to the fact that for free-form surfaces the acquisition and the typical tasks of step 1 and 4 of the 3-D modeling pipeline require human supervision. The only practical way to acquire free-form surface objects is under human supervision, especially if they are valuable and located in museums, churches or, in general, outside of a laboratory. Hole-filling is an inevitable postprocessing step in order to obtain visually pleasing models from data scanned from real objects. Making it automatic is a very difficult problem. For a review of the literature about this topic and an automatic state-of-the-art method see [20]. In this connection one should observe that possibly sizeable holes due to self-occlusions, depending on the object's shape, may be inevitable, and in these cases human supervision may again be necessary. Nevertheless the automatic filling of the small holes is a very important contribution.

With respect to cultural heritage the first contribution of this paper concerns a technique for the completely automatic solution of the first step of the 3-D modeling pipeline, i.e., 3-D views registration. From the technical or conceptual point of view this contribution can be explained as follows. The automatic solution of the pairwise registration of 3-D views requires both the automatic solution of the so called wide-baseline matching problem and the automatic refinement of the pairwise registration parameters, as it will be seen in detail in the next section. For the automatic refinement of the pairwise registration parameters, there is a method universally used under many variants, namely the ICP algorithm [21]. The wide-baseline matching problem is an open research issue, for which nonetheless the literature presents a few automatic solution algorithms. However, the availability of automatic solutions for both issues does not give any guarantee

that their direct combination will work. Indeed it is well known that the ICP algorithm converges only if properly started. There cannot be any guarantee that the parameters produced by any wide-baseline matching technique will always bring to convergence the ICP. The contribution of this work is that it proposes an intermediate step, namely the frequency domain technique of [12], which from the parameters obtained from a wide baseline matching technique is able to generate starting points which always bring the ICP to convergence. As it will be seen these methods are based on rather different principles, which in some sense complement each other. Their combination turns out remarkably robust as its application to cultural heritage shows.

The second contribution of this paper, with respect to cultural heritage, concerns the automatic color restoration and the elimination of photometric artifacts at the seams of different surface patches. The  $(R, G, B)$  texture values are assumed to be in one-to-one correspondence with the range values. This can be obtained by simple portable equipment, such as the standard range camera set up based on a videocamera synchronized with a projector of encoded pattern [22]–[25], which come in many commercial versions in a wide price/performance range. Therefore, the required textures do not need any special equipment or increase of labor, with respect to what would be needed for just acquiring the object's geometry. From a more general technical or conceptual point of view, the interest of the proposed texture processing provisions lays in the fact that they extend notions well established with standard images to colored 3-D surfaces.

A major advantage of the 3-D modeling procedure we propose is its operational simplicity: all one has to do is to make the 3-D scans, from them a textured 3-D model is automatically obtained. All non technical museum personnel would have to know in order to make 3-D models would be to learn how to use a range camera. This is really a minimal and unavoidable requirement in front of the complexity of 3-D modeling real life objects.

This paper is organized in five sections. Section II introduces the techniques suitable to automatize all the phases of the registration process, i.e., the wide-baseline matching, the pairwise registration and the global registration. Section III describes the tools for the removal of the texture's artifacts. It will be seen that the proposed 3-D registration and texture processing methods have strong connections with well known image processing techniques. Section IV presents a number of study cases and a discussion of the proposed method. Section V draws the final remarks.

## II. AUTOMATIC 3-D VIEWS REGISTRATION

The first two steps of the 3-D modeling pipeline traditionally concern the registration of all the 3-D scans of an object, namely the mutual registration of all the pairs of views, called pairwise registration, and the subsequent registration of all the views, called global registration. The registration of a pair of partially overlapping 3-D views is accomplished in two steps: a rough detection of the common region and a fine estimate of the rigid rotation and translation  $(\mathbf{R}, \mathbf{t})$  bringing the two views to the best possible overlap (over the common region). The automatic coarse detection of the common region is an open research area.

It is equivalent to the automatic detection of a number of corresponding points between the two views, therefore it is typically referred to as the wide-baseline matching problem and it is considered in Section II-A. The fine registration of a pair of views is addressed in Section II-B and the global registration in Section II-C.

#### A. Automatic Detection of the Common Region

There exist two fundamental approaches to the automatic detection of a rough common region between a pair of partially overlapping 3-D views. One rests on the use of invariant statistics for each point of the mesh [26]–[32], the other on the use of special features based either on geometry [33]–[36], or on texture [37]. In principle the latter approaches can be more efficient, but less robust (for certain types of objects the wanted features may be missing or not easy to find). All methods, expectedly, have difficulties with highly symmetric objects or parts.

This section reports about the results we obtained with the method of the spin-images introduced by Johnson and Hebert in [31], [32], where the reader is referred for a detailed presentation. The concept of spin-image, here quickly recalled for presentation's clarity, rests upon that of oriented point at a surface mesh vertex, which is defined as the pair formed by the 3-D vertex coordinates and the surface normal at the vertex. Let  $(\alpha, \beta)$  be the coordinates pair defined as follows with respect to the reference system associated to an oriented point: radial coordinate  $\alpha$  is the perpendicular distance to the line through the surface normal at the vertex point, elevation coordinate  $\beta$  is the signed perpendicular distance to the tangent plane defined by vertex normal and position.

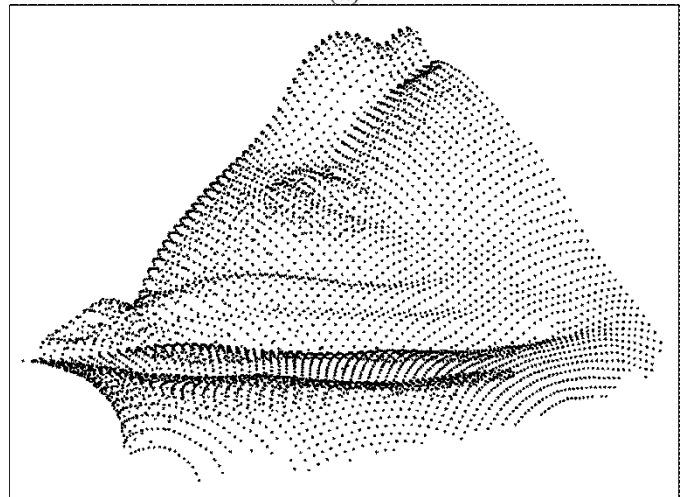
Fig. 1(a) shows a view of a 3-D model of a Pompeian statuette, hereafter called “Lady;” see Table I. Other views of the same object can be seen from Fig. 2. Fig. 1(b) shows the recording of the  $(\alpha, \beta)$  coordinates of all the points of the 3-D mesh of “Lady,” a type of data which we call “spin-map.” A spin-image is a spatially discretized version of a spin-map, where the gray values are associated to the count of points of the spin-map falling in each discrete cell or bin, as shown in Fig. 1(c). The idea of accumulating the points of the spin-map into discrete bins is equivalent to a linear smoothing of the spin-map with an impulse response of value one over the bin and zero elsewhere. Indeed, since spin-images from different 3-D views are used for mutual comparison it is rather useful to remove fine detail and noise in general. For guidelines about mesh simplification and bin's dimensions, see [31].

As Fig. 1 exemplifies, spin-images depend only from the intrinsic surface characteristics (or statistical properties) and not from the surface's spatial position and orientation. In other words the spin-image associated with a vertex point is invariant with respect to rigid rototranslations.

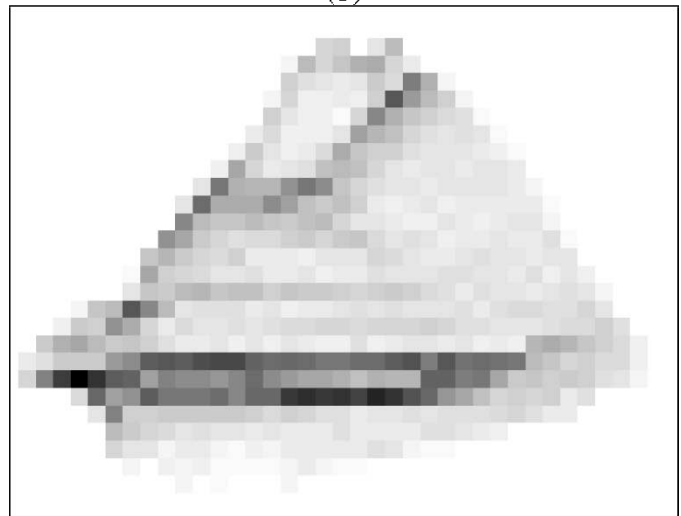
It is also very important to observe that the spin-images of neighbor points are very similar because the features of the local surface area near the point have a greater impact in the spin-image formation. Therefore, by way of spin-images, one may associate a collection of images to a 3-D surface mesh, as every point of the surface can generate a spin-image. A pair of surfaces representing the same object from different view-points



(a)



(b)



(c)

Fig. 1. Lady: (a) single 3-D view, (b) spin-map, and (c) spin-image.

will be associated to a pair of sets of different spin-images: corresponding points in the common region between two 3-D views

TABLE I  
DATA ABOUT “LADY”

“Lady”	
Height	187.9 mm
Total no. of scans	24
Memory occupancy of a single scan (PIF format)	1.659 Mb
Memory occupancy of the whole VRML model	57,7 Mb
Texture type	RGB
Average displacement error	4.32 mm
Average pair-wise registration error	0.402 mm
Average execution time	27.40 s
Final registration error	$3.405 \cdot 10^{-4}$ mm
Average triangle side	0.217 mm
Total number of triangles	2084308
Total surface area	12996.08 mm <sup>2</sup>

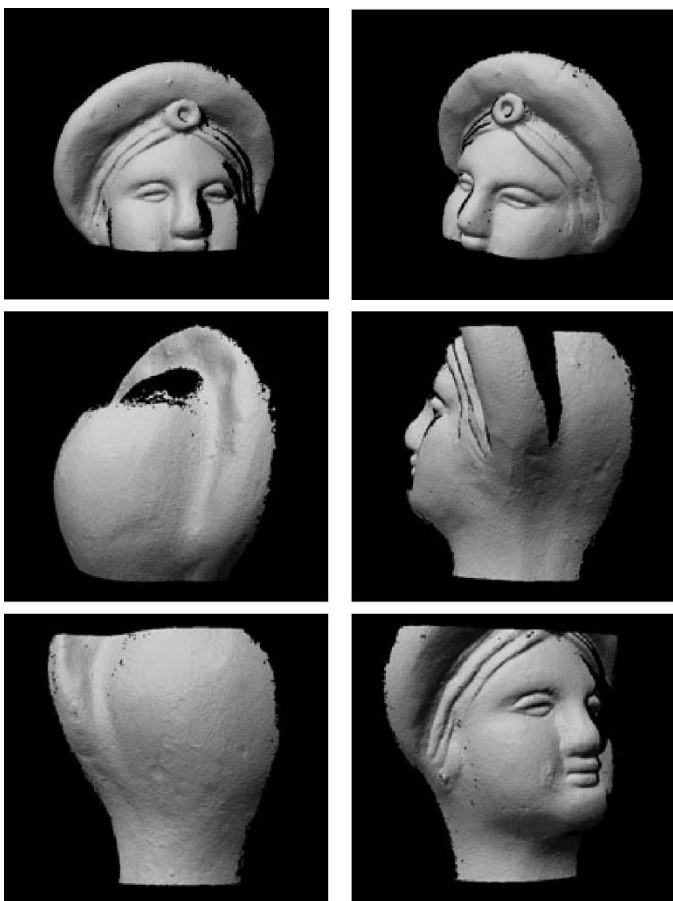


Fig. 2. Six of the 24 scans of “Lady.”

will have similar spin-images because, as already pointed out, spin-images strongly depend on local shape’s characteristics. The spin-images of corresponding points of two partially overlapping 3-D views will not be identical because of surface discretization effects and because the two patches share only a portion of their surface. However, if the overlap is substantial (no

less than 30% of regions characterized by an adequate presence of geometrical features) corresponding points of the two 3-D views located in the common region will have similar spin-images. The detection of the common region between two partially overlapping 3-D views in this way can be turned into the recognition of the most similar images of two sets of (spin) images, a problem for which a number of techniques are available.

The procedure for detecting corresponding points is shown in Fig. 3. A set of putative point correspondences is determined upon the similarity of the spin-images. The correspondences are verified against basic distance invariance constraints, i.e., if  $\mathbf{p}_1$  and  $\mathbf{p}_2$  are two points of the first mesh and  $\mathbf{q}_1$  and  $\mathbf{q}_2$  are their putative correspondences in the second mesh, they are retained only if  $\|\mathbf{q}_1 - \mathbf{q}_2\| - \varepsilon < \|\mathbf{p}_1 - \mathbf{p}_2\| \leq \|\mathbf{q}_1 - \mathbf{q}_2\| + \varepsilon$  with a suitable  $\varepsilon$ . Fig. 4 shows the set of correspondences between two of the 3-D scans shown in Fig. 2 determined by the most similar spin-images: the ones not complying with the distance preservation constraint will be rejected.

The correspondences are organized within groups and for each group one determines the roto-translations  $(\mathbf{R}, \mathbf{t})$  moving the points of the first 3-D view as close as possible to their corresponding points in the second 3-D view, via Horn’s algorithm [38]. The roto-translation  $(\mathbf{R}, \mathbf{t})$  giving the widest overlap between the two views is selected. The common region between the two views is taken to be this overlapping area.

Fig. 5 shows the estimated common region between the two views of Fig. 4. Fig. 6(a) shows the rough alignment of the two 3-D views of Fig. 4 obtained by bringing to coincidence the corresponding points found by the spin-images method. The geometrical artifacts due to the poor estimate are clearly noticeable in the central part of the face; see, for instance, the doubling of the Lady’s little disk (in the middle of the front) and nose.

Our implementation followed [32] with minor practical fixes. In presence of at least 30% surface’s overlap over adequately characterized regions, this method was always able to find an approximate but correct common region. The precision of the detected overlap may vary in dependence of the actual object shape.

### B. Automatic Pairwise Registration of 3-D Views

The final estimate of the rotation and translation  $(\mathbf{R}, \mathbf{t})$  between two 3-D views is typically accomplished by the ICP algorithm [21] or some of its variants [39]–[44]. The rough pre-alignment obtained by spin-images is often adequate to bring the ICP to convergence. However this was not found to be always the case, consistently with the fact that the ICP algorithm is known to be able to produce very precise estimates of  $\mathbf{R}$  and  $\mathbf{t}$  when properly started, as it may otherwise be trapped by local minima. This problem may be overcome by initiating the ICP from different starting points, a strategy for their selection is proposed in [45]. In practice, this issue is commonly solved by manually selecting a few corresponding points from which an estimate of  $(\mathbf{R}, \mathbf{t})$  is determined by Horn’s algorithm.

In order to have a fully automatic procedure we use instead the frequency domain method of [12] as a robust device for determining a first estimate of the  $(\mathbf{R}, \mathbf{t})$  parameters to use as starting point for the ICP (there are also other reasons for using this technique, as it will become clear momentarily). The

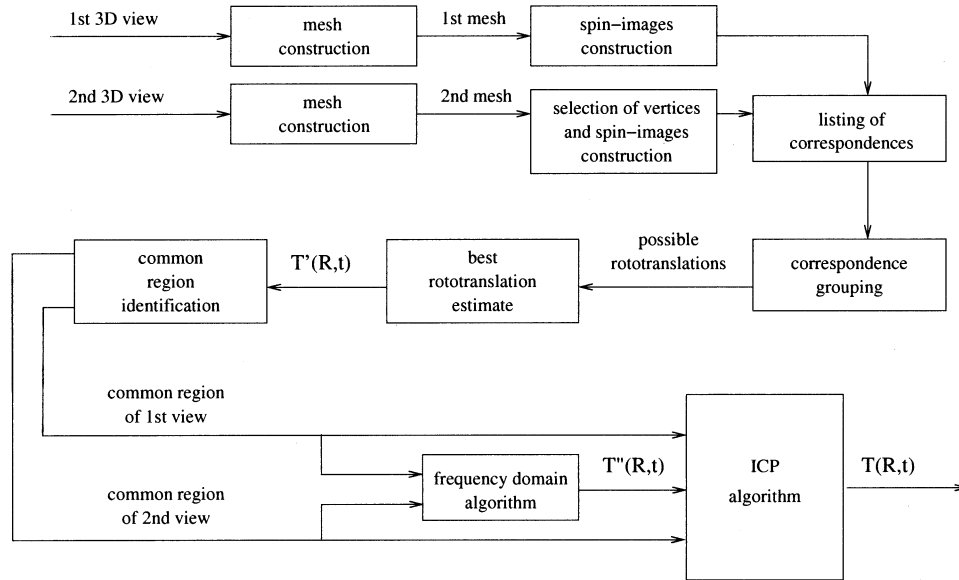


Fig. 3. Algorithm for the automatic registration of a pair of 3-D views.

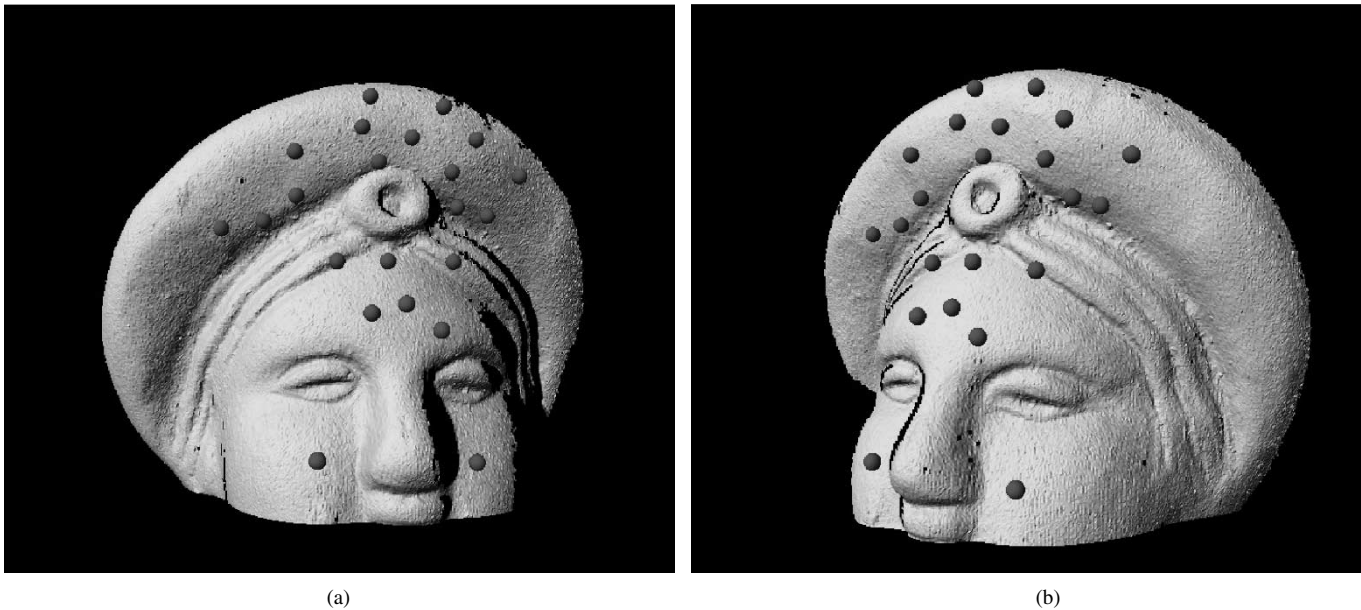


Fig. 4. Example of putative correspondences between two partially overlapping meshes.

method of [12] and the ICP operate on very different principles and their combination turns out remarkably robust. It may be worth recalling the rationale of both methods in order to motivate their synergy.

If textured surface  $l_2(\mathbf{x})$  is a version of  $l_1(\mathbf{x})$  rigidly rotated and translated by  $(\mathbf{R}, \mathbf{t})$ , i.e.,

$$l_2(\mathbf{x}) = l_1(\mathbf{R}^{-1}\mathbf{x} - \mathbf{t}) \quad (1)$$

the Fourier transform of  $l_1(\mathbf{x})$  and  $l_2(\mathbf{x})$ , respectively denoted as  $L_1(\mathbf{k})$  and  $L_2(\mathbf{k})$  are related as

$$L_2(\mathbf{k}) = L_1(\mathbf{R}^{-1}\mathbf{k})e^{-j2\pi\mathbf{k}^T\mathbf{R}\mathbf{t}}. \quad (2)$$

In terms of magnitudes, (2) simplifies in

$$|L_2(\mathbf{k})| = |L_1(\mathbf{R}^{-1}\mathbf{k})|. \quad (3)$$

It can be proved [12] that the versor of the rotation axis, is the vector  $\mathbf{k}$  which equates to 0 the difference function

$$\Delta(\mathbf{k}) = \left| \frac{|L_1(\mathbf{k})|}{L_1(\mathbf{0})} - \frac{|L_2(\mathbf{k})|}{L_2(\mathbf{0})} \right| = \left| \frac{|L_1(\mathbf{k})|}{L_1(\mathbf{0})} - \frac{|L_1(\mathbf{R}^{-1}\mathbf{k})|}{L_1(\mathbf{0})} \right|. \quad (4)$$

An effective technique to solve this minimization problem is given in [12], together with a procedure for estimating the rotation angle upon the rotation axis, and the translation vector  $\mathbf{t}$  upon knowledge of  $\mathbf{R}$ .

We want to point out that the frequency domain algorithm of [12] does not operate on a point-to-point correspondence logic as the ICP, since the Fourier transform makes a synthesis of all the available spatial information. Furthermore, since the Fourier transform doesn't only take into account the 3-D shape informa-

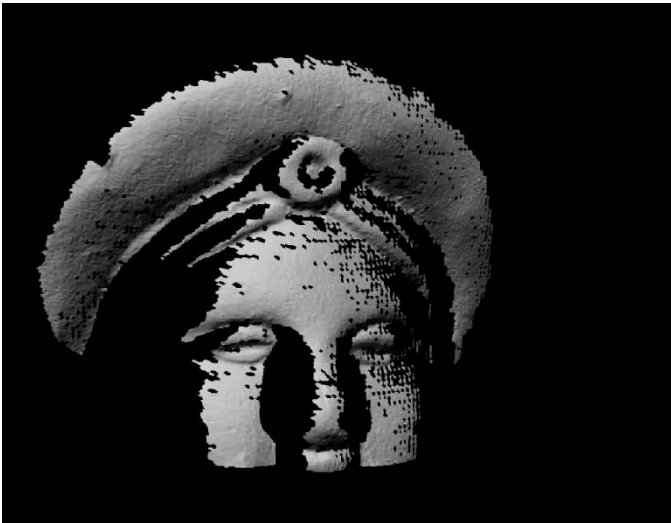


Fig. 5. Common region between the two views of Fig. 4 automatically determined by the spin-images method.

tion, but also the texture information, the method of [12] is able to register textured symmetrical objects (such as painted vases, that could not be aligned on the basis of local geometrical information only). This possibility, as it will be seen, plays a rather valuable service for practical modeling of heritage's objects.

Since the frequency domain method does not operate directly on the 3-D surface data, but it has to turn them into small volumes in order to avoid the singularity issues related to the Fourier transform of 3-D signals supported by 2-D manifolds, it is not as precise as the ICP, which directly operates on spatial point-wise correspondences. It is also fair to add that, in general, the alignment obtained by the frequency domain method is already satisfactory, not only because it differs very little from the refinement obtained by the ICP, but also because a further global registration pass, described in Section II-C, is needed in any case.

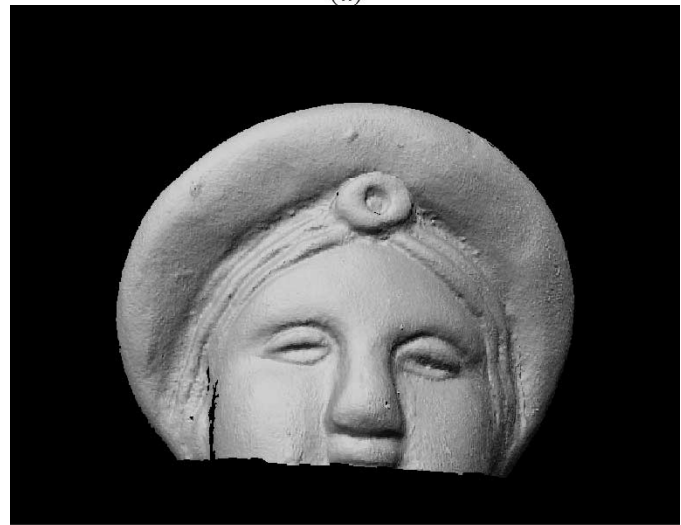
As well known, the general idea behind the ICP algorithm is to find sets of matching points on the overlap of the two 3-D views by minimizing the distance between the points of a 3-D view and a candidate set of corresponding points in the other view, in the Euclidean sense or according to more efficient but conceptually similar geometrical criteria. It can be proved that this procedure suitably iterated converges to a local minimum [21]. For completeness we should also add that there exist an extension of the ICP which operates on the basis of geometry and texture information [46].

### C. Global Registration

The full coverage of an object typically requires many more than just two 3-D views, depending on the object's articulation, size and on the model's spatial resolution. The pairwise registration procedure, even in front of very accurate results for each pair of 3-D views, cannot model full objects because of error accumulation. The errors may come from the pairwise registration procedure itself as well as from measurement noise and discretization effects on the acquired surface. Fig. 7(a) shows the result of the pairwise registration of all the views of "Lady." The misalignment artifacts are evident.



(a)



(b)

Fig. 6. (a) Automatic prealignment by the spin-images method. (b) Final pairwise registration by the frequency domain method followed by the ICP.

There are several methods for redistributing the registration errors upon the results produced by a pass of pairwise 3-D views registration, such as [47]–[50], for recent literature reviews see [6], [51].

We have direct experience with the methods of [49] and [50]. The algorithm of [50] can reach good quality global alignments, but only after many iterations and as the total number of 3-D views increases, the total iterations number increases and the computation time and memory allocation per single iteration increase. The global registration technique of [49] reaches global registration of comparable quality with much better memory/speed performance. This algorithm indeed was successfully applied to the global registration of large models of statues [3].

Fig. 7(b) shows the model of "Lady" after global registration by the method of [49], the improvement over the model obtained simply by pairwise registration is evident. The actual registration data and modeling results are discussed in Section IV.



(a)



(b)

Fig. 7. The 3-D model after (a) pairwise registration and (b) global alignment.

### III. TEXTURE PROCESSING

The texture problems we encountered in 3-D modeling were essentially of two types: textures presenting colors different from those of the actual objects and photometric differences at the seams of different 3-D surface patches. The first type of artifacts is fairly common in photographic processes as the responses of films or digital sensors to light cannot perform the adjustments typical of human perception (color constancy). The second type of artifacts in our cases was due to non uniform lighting conditions, which are practically inevitable with nonflat objects. Furthermore, photometric imbalances are, to a certain extent, common of image compositing because of vignetting (the fact that the light intensity collected by the photographic optics at the image borders is lower than at the image center). We used the color texture correction method of [52] in order to restore actual color appearance and an “ad hoc” color blending procedure in order to handle major photometric imbalances between adjacent surface patches.



(a)



(b)

Fig. 8. (a) View of the final textured model (b) a picture of the actual statue.

The color texture correction of [52] estimates the average illumination of an image from its  $(R, G, B)$  values upon statistical arguments. This is obtained by assuming uniform, i.e., space independent, illumination, by associating to each  $(R, G, B)$  value of the image the spectrum of the color of the Munsell's atlas [53] closest to it and by assuming that the second order statistics of the reflectances of the object coincides with the second order statistics of all the colors of the Munsell's atlas. The illuminant's estimate is obtained by singular value decomposition of the logarithms of the spectra, a framework reminiscent of homomorphic signal processing. The associated inverse filtering problem is solved by standard regularization techniques.

Fig. 9(a) shows the model of a paleovenetical “situla,” a special type of bronze vase of the 7th century B.C., whose color in the acquired textures turned out much browner than that of the actual object. Furthermore, the model exhibits some minor photometric differences, partly due to vignetting, at the seams of adjacent patches [clearly evidenced in the detail of Fig. 9(b)]. Fig. 10(a) shows a situla's detail with the right color; Fig. 10(b)

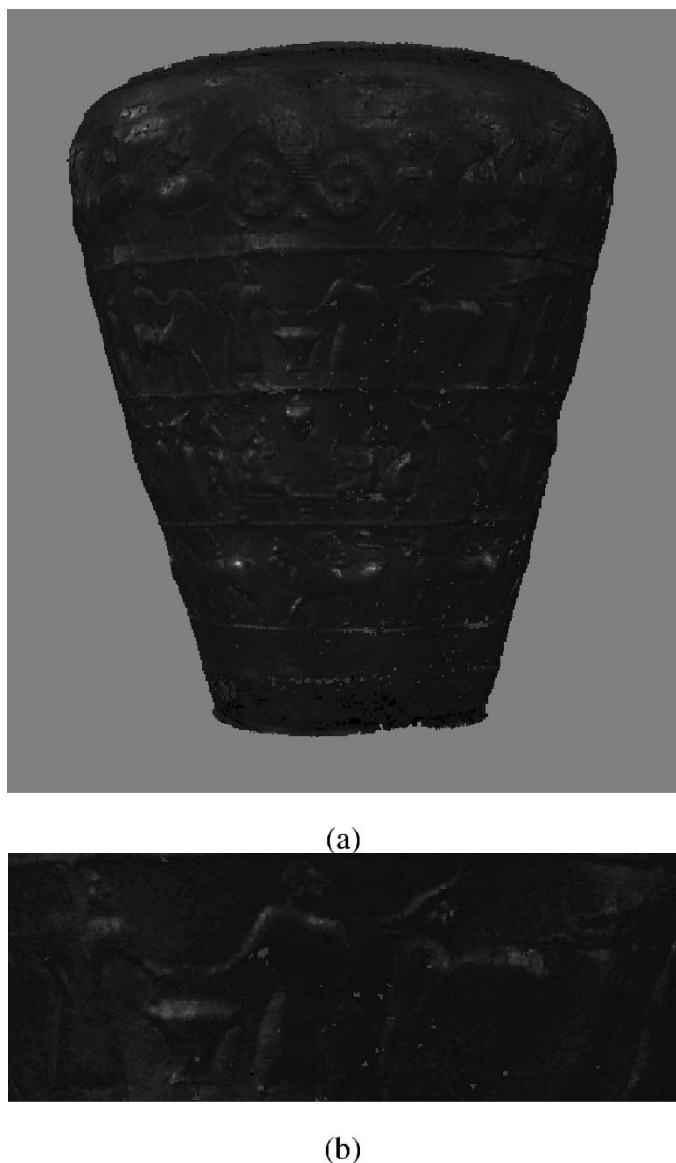


Fig. 9. (a) View of the model of a situla obtained without texture processing and (b) detail.

shows an example of actually acquired texture patch characterized by its brownish color; and Fig. 10(c) shows the patch of Fig. 10(b) equalized with respect to the colors of the patch of Fig. 10(a). The actual results, also shown in Fig. 11, are discussed in Section IV.

The tool we used against major photometric imbalances is a texture blending procedure for 3-D surfaces which was inspired by [54] and by the color blending procedure of [55] subsequently revisited within a wavelets framework in [56].

Fig. 12 shows the model of an Attic vase (V century b.C.), directly built from the acquired textures, clearly exhibiting strong nonuniform illumination effects. The task of the color blending procedure is to assign an  $(R, G, B)$  value to each pixel of the common regions between different 3-D views, which, as such, has as many candidate  $(R, G, B)$  values as the number of overlapping patches. For clarity's sake we introduce the color blending procedure with the aid of an example shown in Fig. 13. Fig. 13(a) and (b) show the range data of a pair of

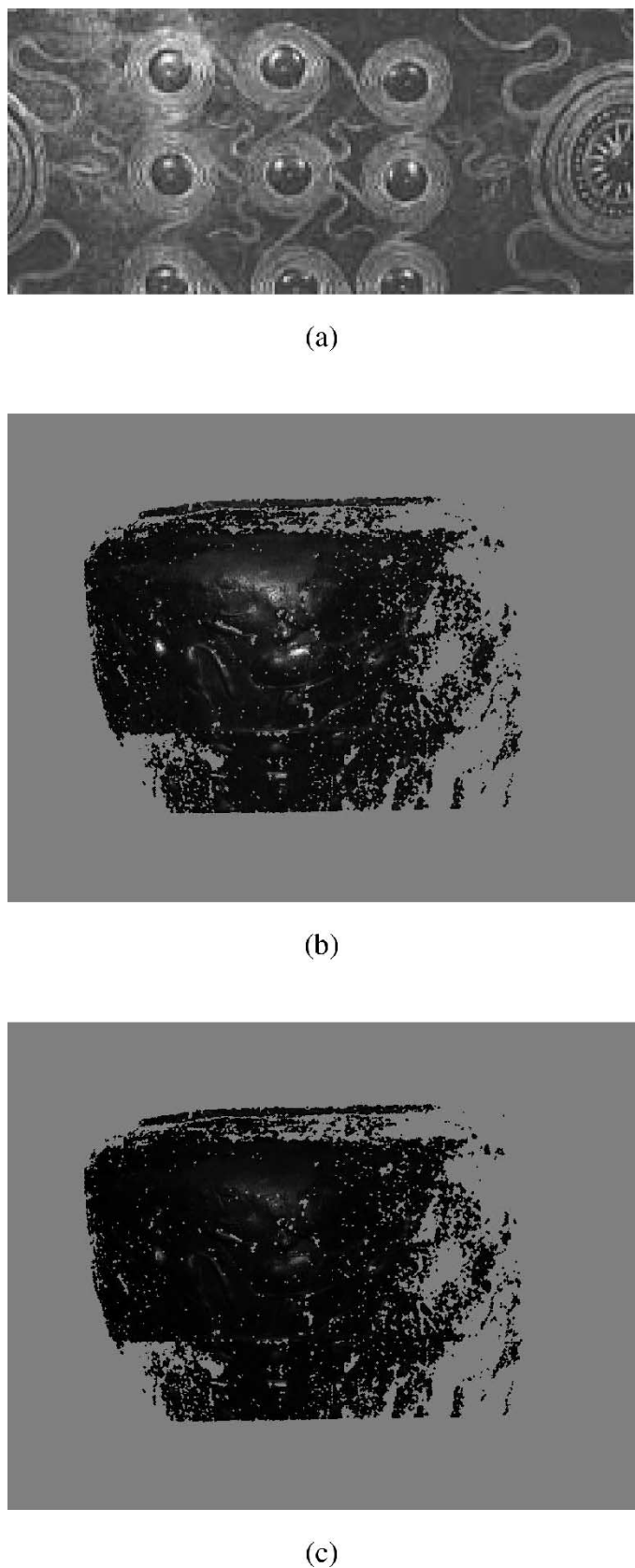


Fig. 10. (a) Detail of the situla with proper color, (b) surface patch with wrong color, and (c) surface patch color corrected.

partially overlapping scans of the Attic vase and Fig. 13(c) and (d) the relative textures. Fig. 13(e) shows the common region



(a)



(b)

Fig. 11. View of the model of the situla obtained after textures were color corrected by the method of [52].

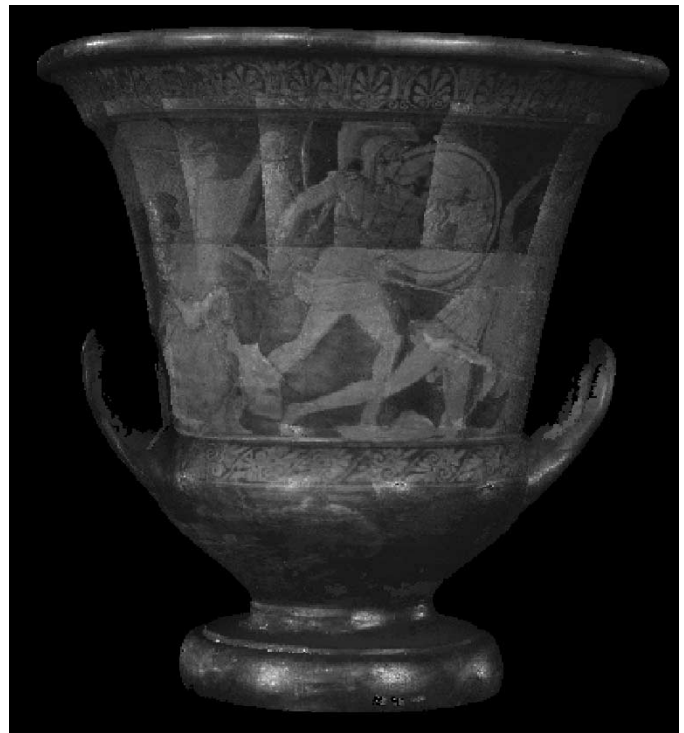
from the texture of Fig. 13(c), i.e., the surface's region such a texture shares with the texture of Fig. 13(d). Since we operate on already registered 3-D views, the use of 3-D information makes straightforward the localization of the mutual common region between textures and the detection of the intervening textures.

Fig. 13(f) shows the remapping of the common region from the texture of Fig. 13(d) on the texture of Fig. 13(c). More precisely Fig. 13(f) is obtained by the following procedure:

#### Lateral remapping:

Repeat for each pixel  $p = (x, y)$  of the texture of the common region between two laterally overlapping surface patches:

- Pick  $p = (x, y)$  from the left texture (Fig. 13(c));
- Consider the corresponding 3-D point in the associated range data (Fig. 13(a));
- Determine the range point closest to it in the



(a)



(b)

Fig. 12. (a) View of the model of an Attic vase obtained without texture processing and (b) detail of the back side.

mesh of the right 3-D view (Fig. 13(b));

Find the corresponding pixel value in the right texture (Fig. 13(d));

Write this (R,G,B) value at position  $p = (x, y)$  of the remapped texture (Fig. 13(f));

End of Lateral remapping

The remapped texture of Fig. 13(f) shows some artifacts because of discretization, indeed not all the pixels of the left spatially discretized texture have a correspondent pixel in the right spatially discretized texture. Spatially continuous textures instead would give perfect correspondence and no consequent visual artifact. Fig. 13(g) shows in white the support of the common region between the left and right textures of Fig. 13(e) and Fig. 13(f), respectively.

A binary mask for the common region is determined by the following procedure:

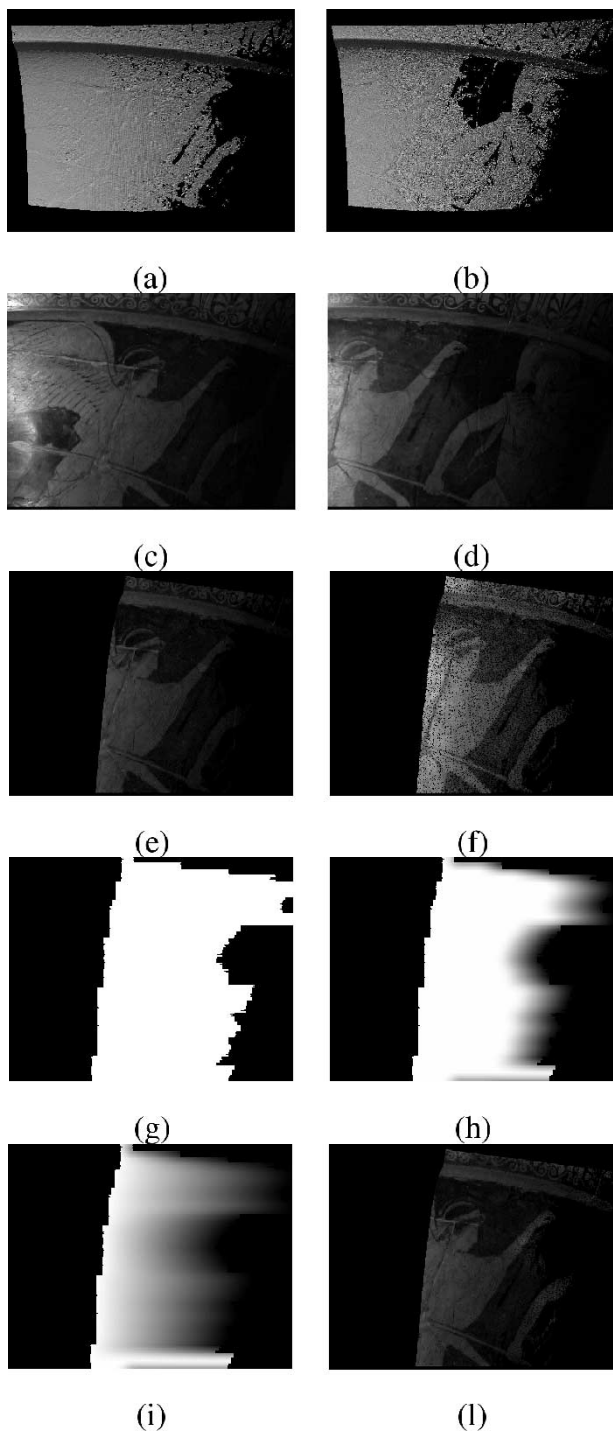


Fig. 13. (a) Range view and (c) corresponding texture. (b) Range view and (d) corresponding texture. (e) Common region from the texture of Fig. 13(c). (f) Common region from the texture of Fig. 13(d) remapped on the texture of Fig. 13(c). (g) Mask. (h) Choice for the weight coefficients. (i) Another choice for the weight coefficients. (j) Blended texture.

**Horizontal mask:**

Repeat for each row of the image of the common region:

- Determine the position  $x_1$  of the left border and the position  $x_2$  of the right border of the common region;
- Assign  $a = x_1 + (2/3)(x_2 - x_1)$ ,  $b = x_2$ ;

Form the mask image by setting the value  $p(x)$  of the generic pixel at location  $x_1 \leq x \leq x_2$  of the row as follows:

- If  $x \leq a$  then  $p(x) = 1$ ;
- If  $a < x < b$  then  $p(x) = 1 - (x - a)/(b - a)$ ;
- If  $x \geq b$  then  $p(x) = 0$ ;

End of Horizontal mask

A weight image, shown in Fig. 13(h), is determined by filtering row-wise the mask image. By using other rules for the values of the  $a$  and  $b$  parameters which determine the ramp's beginning and end, other masks and weight images can be obtained. We tried many other assignment rules, for instance Fig. 13(i) shows the mask produced by setting  $a = x_1$  and  $b = x_2$  in procedure "Horizontal mask".

The positions of the projector, videocamera and of the lights of our acquisition systems were fixed. The geometry of the Attic vase was such that all the acquired textures exhibited a strong illumination peak at the left side. We experimentally found that the mask of Fig. 13(h) obtained with the assignment rules specified in procedure "Horizontal mask" were the most appropriate for the type of nonuniform illumination exhibited by the textures actually acquired for the Attic vase. The mask of Fig. 13(h) indeed weights the color values of the left texture (which, at its right, side is not affected by any illumination peak) much more than those of the right texture, thus avoiding the illumination peaks typical of the left side of the right textures of the Attic vase. With textures more uniformly illuminated, a different assignment rule for parameters  $a$  and  $b$ , such as the one leading to the weights of Fig. 13(i), may be more appropriate. The illumination's distribution depends both on the object's geometry and on the characteristics of the acquisition set-up.

The blended texture values are determined by the following procedure:

**Color blending:**

For each pixel  $p = (x, y)$  of the common region:

- Consider the corresponding color  $C_1 = (R_1, G_1, B_1)$  of the left texture (Fig. 13(c));
- Consider the corresponding color  $C_2 = (R_2, G_2, B_2)$  of the remapped right texture (Fig. 13(f));
- Consider the corresponding scalar weight  $w$

(Fig. 13(h));

Assign to the pixel  $p = (x, y)$  of the blended texture the color  $C = w * C_1 + (1 - w) * C_2$ ;

End of Color blending

The above texture blending procedure is first applied row-wise to all the "belts" of partially horizontally overlapping surface patches, then it is applied vertically to all the surface patches with partial vertical overlaps. The mask images for the vertical overlaps are obtained by a procedure very similar to the one used for the masks of the horizontal overlaps, except that the procedure operates column-wise. The weight images are obtained by filtering the mask images along the columns.

We also tried blending according to a four channel wavelet decomposition of mask image and of each one of the two textures as suggested in [56], but the difference between the results produced by this much more computationally intensive procedure and the simpler single channel convex combination procedure just presented were never appreciable. The next section discusses the actual performance of this method.

#### IV. EXPERIMENTAL RESULTS AND DISCUSSION

This section discusses a few practical examples of automatic modeling of textured objects by the tools described in Section II and III.

As first example, we consider the automatic modeling of "Lady" introduced in Section II. Some data about this piece are reported in Table I. The spin-images method was able to automatically find the common regions between all the pairs of partially overlapping 3-D scans and to preliminarily align them by bringing to coincidence the common regions as shown in Fig. 6(a) for a pair of upper scans. Table II reports the execution times on a Pentium III 1.8 GHz, which are between 15.27 s and 43.66 s. The spread in the execution times depends on the number of object's points in each scan; the greater is the number of object's points the longer is the execution time, since there are more spin-images to generate and process. Note that in the Parametric Image Format (PIF) file the scan's dimension are independent of the object's point actually represented. For a description of PIF format, see [57]. The displacement error of a single point is the distance between its position after the prealignment by way of spin-images and its final position after global registration. The values reported in Table II are the averages of the displacement errors of all the points in each common region. The spread in the displacement errors is due to the error accumulation of the pairwise alignment procedure. This is clearly shown by the increase of this error from 0.97 mm to 7.43 mm found in the sequential registration of the adjacent scans of the upper belt labeled with increasing integers from L00.pif to L10.pif.

Table II also reports the average registration error between corresponding points for each pair of overlapping 3-D views, prealigned by the spin-images method. The values of these data are rather uniform. This indicates a regular performance of the spin-images method with data with uniform characteristics. The comparison of the average registration error after the prealignment by way of spin-images with the average registration error after global registration, which is reported in Table I, indicates that they are about three orders of magnitude greater. Table II reports also the average side of the mesh of triangles of the model's surface, the total number of triangles and the surface's area.

Since the spin-images method operates on pairs of scans, the proposed procedure can be applied to objects acquired by any number of scans provided that the overlap between the scans is around 30% and that the common region be adequately characterized (so that the spin-images may have adequate features to exhibit). This means that one must exercise some care during the taking in order to scan according to the above requirements:

TABLE II  
EXECUTION TIMES AND REGISTRATION ERRORS OF THE PREALIGNMENT BY THE SPIN-IMAGES

"Lady": times and errors				
1st 3D view	2nd 3D view	Time	Displacement error	Registration error
L00.pif	L01.pif	43.66 s	0.97 mm	0.414 mm
L01.pif	L02.pif	34.71 s	2.18 mm	0.381 mm
L02.pif	L03.pif	19.36 s	2.53 mm	0.416 mm
L03.pif	L04.pif	15.27 s	2.83 mm	0.409 mm
L04.pif	L05.pif	21.72 s	3.37 mm	0.429 mm
L05.pif	L06.pif	25.88 s	3.80 mm	0.439 mm
L06.pif	L07.pif	29.16 s	4.40 mm	0.414 mm
L07.pif	L08.pif	25.78 s	5.40 mm	0.387 mm
L08.pif	L09.pif	17.38 s	6.87 mm	0.347 mm
L09.pif	L10.pif	15.41 s	7.51 mm	0.412 mm
L10.pif	L11.pif	23.80 s	7.43 mm	0.331 mm
L00.pif	L12.pif	36.07 s	0.60 mm	0.394 mm
L01.pif	L13.pif	40.84 s	0.16 mm	0.412 mm
L02.pif	L14.pif	29.76 s	1.77 mm	0.358 mm
L03.pif	L15.pif	16.59 s	4.18 mm	0.415 mm
L04.pif	L16.pif	24.02 s	5.12 mm	0.434 mm
L05.pif	L17.pif	29.20 s	6.71 mm	0.409 mm
L06.pif	L18.pif	27.73 s	4.47 mm	0.390 mm
L18.pif	L19.pif	28.58 s	7.63 mm	0.413 mm
L19.pif	L20.pif	31.86 s	6.53 mm	0.418 mm
L20.pif	L21.pif	32.45 s	6.60 mm	0.394 mm
L21.pif	L22.pif	30.38 s	6.51 mm	0.388 mm
L22.pif	L23.pif	30.69 s	6.99 mm	0.396 mm
Average values		27.40 s	4.35 mm	0.402 mm

examples of 3-D scans with adequate mutual overlaps are shown in Fig. 2.

The results of the pairwise alignment of all the 24 views are shown in Fig. 7(a) versus the final model, obtained after the global registration, shown in Fig. 7(b). Fig. 7(a) makes clear the limits of the pairwise alignment even with a small number of views (i.e., 24), as in the case of "Lady." However, as shown in Fig. 7(b), the global alignment, is able to determine the millimetric point displacements needed to overcome the misalignment problems (their average values are reported in Table II). In light of this fact one can appreciate that the accuracy of the pairwise registration is somewhat secondary with respect to that of the global registration technique, and that the accuracy of the frequency domain technique, although not as high as that of the ICP, as reported in [12], is nevertheless adequate for the pairwise alignment's purposes.

All the textures of "Lady" were equalized by the technique of [52].

As Fig. 8 shows, the model is visually coherent both geometrically and colorimetrically with the original. The differences between the actual picture of the original object shown in Fig. 8(b) and the view of the 3-D model of Fig. 8(a), are mostly

TABLE III  
DATA ABOUT THE ETRUSCAN SKULL

"Etruscan Skull"	
Height	154.28 <i>mm</i>
Total no. of scans	17
Memory occupancy of a single scan (PIF format)	6.32 Mb
Memory occupancy of the whole VRML model	58.6 Mb
Texture type	-
Average displacement error	5.82 <i>mm</i>
Average pair-wise registration error	0.813 <i>mm</i>
Average execution time	46.81 <i>s</i>
Final registration error	$1.536 \cdot 10^{-3}$ <i>mm</i>
Average triangle side	0.548 <i>mm</i>
Total number of triangles	741358
Total surface area	76690 <i>mm</i> <sup>2</sup>

TABLE IV  
EXECUTION TIMES AND REGISTRATION ERRORS OF THE PREALIGNMENT BY THE SPIN-IMAGES

"Etruscan Skull": times and errors				
1st 3D view	2nd 3D view	Time	Displacement error	Registration error
S00.pif	S01.pif	07.62 <i>s</i>	0.93 <i>mm</i>	0.908 <i>mm</i>
S01.pif	S02.pif	09.30 <i>s</i>	1.67 <i>mm</i>	0.913 <i>mm</i>
S02.pif	S03.pif	15.88 <i>s</i>	1.83 <i>mm</i>	0.916 <i>mm</i>
S03.pif	S04.pif	32.91 <i>s</i>	2.76 <i>mm</i>	0.734 <i>mm</i>
S04.pif	S05.pif	63.85 <i>s</i>	3.76 <i>mm</i>	0.779 <i>mm</i>
S05.pif	S06.pif	88.44 <i>s</i>	5.39 <i>mm</i>	0.808 <i>mm</i>
S06.pif	S07.pif	71.27 <i>s</i>	9.34 <i>mm</i>	0.817 <i>mm</i>
S07.pif	S08.pif	55.10 <i>s</i>	12.78 <i>mm</i>	0.803 <i>mm</i>
S08.pif	S09.pif	43.83 <i>s</i>	27.45 <i>mm</i>	0.810 <i>mm</i>
S00.pif	S14.pif	08.69 <i>s</i>	1.90 <i>mm</i>	0.86 <i>mm</i>
S14.pif	S13.pif	17.65 <i>s</i>	2.29 <i>mm</i>	0.948 <i>mm</i>
S13.pif	S12.pif	46.94 <i>s</i>	2.19 <i>mm</i>	0.802 <i>mm</i>
S12.pif	S11.pif	59.78 <i>s</i>	2.53 <i>mm</i>	0.783 <i>mm</i>
S11.pif	S10.pif	52.28 <i>s</i>	12.81 <i>mm</i>	0.856 <i>mm</i>
S05.pif	S15.pif	86.48 <i>s</i>	5.81 <i>mm</i>	0.642 <i>mm</i>
S05.pif	S16.pif	88.88 <i>s</i>	5.43 <i>mm</i>	0.627 <i>mm</i>
Average values		46.81 <i>s</i>	5.82 <i>mm</i>	0.813 <i>mm</i>

due to the flash light used in the actual taking of the picture (which produces a kind of uniform strong illumination not easy to emulate with synthetic lights) and to a much lesser extent to the approximate replica of the picture's viewpoint.

As a second study case we consider the model of an Etruscan skull, found in a tomb. This object was acquired without texture since we were told that only its geometry is of anthropological archaeology's interest. The basic data about this object are given

TABLE V  
DATA ABOUT SITULA

Situla	
Height	331.5 <i>mm</i>
Total no. of scans	52
Memory occupancy of a single scan (PIF format)	6.32 Mb
Memory occupancy of the whole VRML model	173 Mb
Texture type	RGB
Final registration error	$3.74 \cdot 10^{-4}$ <i>mm</i>
Average triangle side	0.533 <i>mm</i>
Total number of triangles	2108331
Total surface area	235217.3 <i>mm</i> <sup>2</sup>

TABLE VI  
DATA ABOUT ATTIC VASE

Attic Vase	
Height	651.1 <i>mm</i>
Total no. of scans	72
Memory occupancy of a single scan (PIF format)	6.32 Mb
Memory occupancy of the whole VRML model	328 Mb
Texture type	RGB
Final registration error	$1.147 \cdot 10^{-3}$ <i>mm</i>
Average triangle side	0.547 <i>mm</i>
Total number of triangles	4165765
Total surface area	475310.8 <i>mm</i> <sup>2</sup>

by Table III. Fig. 15(a) shows some 3-D scans and Fig. 15(b) shows a view of the full model.

Table IV reports the data concerning the prealignment by the spin-images method. The average execution time is about twice the average execution time of "Lady," since the scans have a much greater number of object's points (as indirectly indicated by the dimensions of the .PIF files, which for the skull are 6.32 Mb, see Table III, and for "Lady" are 1.65; see Table I). The average displacement error of the skull is comparable with that of "Lady" in spite of a couple of views concerning the back of the skull with high displacement error peaks, due to their specific characteristic (both have about constant curvature).

As a third study case we consider the situla shown in Fig. 9 and Fig. 11. Table V gives some data about this object. This situla is too symmetrical to be automatically prealigned by the spin-images method. The spin-images are not sensitive enough to the fine relief decoration of this vase. However this fact is not at all a practical problem for the automatic alignment of this object or more in general for objects characterized by a high degree of symmetry, such as vases and similar. Indeed it is rather natural to scan this type of objects in a regular way, for instance row-wise and left-to-right keeping the same overlap between adjacent views, and once a row is completed to continue with a vertically adjacent row with a prescribed overlap with respect to the above one. In this way the prealignment by way of the spin-images can be bypassed by the a-priori knowledge about the mutual position of the 3-D scans granted by the taking procedure. In practice the coarse prealignment obtained by the spin-images method can be replaced by a suitable labeling of the 3-D scans.



(a)



(b)

Fig. 14. View of the model obtained after the textures were color corrected by the method of [52] and blended by the procedure of Section III.

Once the common region is determined, the frequency domain method can refine the pairwise alignment from geometry and texture information and the global alignment method, from the geometrical information, is able to determine the fine shifts needed for a proper alignment. As Table V indicates, final registration error of the situla's 3-D model is  $3.74 \cdot 10^{-4}$  mm.

As anticipated in Section III, the situla's modeling difficulties were not related to the reproduction of its geometry but of its



(a)



(b)

Fig. 15. Etruscan skull. (a) Some 3-D scans and (b) a view of the model.

color. We were forced to scan within a room without any window and the lights we had produced textures of the wrong color. Another acquisition session at another time would have implied costs both for the museum personnel scheduled to help us and for us, since we were out of town. Therefore we decided to digitally correct the colors in our lab. Fig. 9 shows a view of the situla's model obtained without any texture processing: the bronze looks brownish while its actual color is much greener, furthermore the model exhibits some light photometric discontinuities between different patches [see the detail of Fig. 9(b)] due to vignetting. Fig. 12 shows a view of the model obtained after all the textures were color corrected by the method of [52] with respect to the reference image of Fig. 10(a). As it can be seen the situla's bronze recovered its natural green color as shown by Fig. 11 and the photometric differences disappeared without further texture blending.

As a fourth study case, we consider the Attic vase, shown in Fig. 12 and subsequent. Table VI reports some data about this object. The geometrical symmetry of this object makes it unsuited to determine the common regions by the spin-images method. Nevertheless, its automatic alignment can be obtained as explained for the situla. The possibility, given by the frequency domain technique, of exploiting texture information, in

this case turns out rather useful. The final registration error of the Attic vase's model is  $1.147 \cdot 10^{-3}$  mm.

It was not possible to acquire the interior of the vase's handles with the equipment we had at acquisition times. We had mirrors with us but their dimension would not fit within the handles. We were told that the handles were secondary with respect to the whole vase's geometry and decoration. So we decided to fix them by manual postprocessing and to leave them out of our actual measurements. Since our figures refer to 3-D models automatically built from actual scans without manual postprocessing, the vase is shown with incomplete handles.

As explained in Section III, the vase's dimensions are such that with our 3-D imaging system all the acquired textures were strongly illuminated at their left. The photometric artifacts of the model of the Attic vase directly obtained from the acquired textures are extremely noticeable, as Fig. 12 shows. The texture blending procedure of Section III was able to remove the color discontinuities and to restore the proper texture as shown in Fig. 14.

## V. CONCLUSIONS

This work presents a technique for the automatic realization of textured 3-D models of objects from scans of synchronized texture and depth images, provided also by current low-cost range cameras based on the projection of encoded patterns.

Specific points of interests of the proposed methods are the use of the frequency domain technique of [12] as a robust device for the automatic determination of effective starting points of the ICP algorithm upon the crude registration parameters obtained from the method of the spin-images and the procedures for obtaining a full artifact-free texture of the object, simply from color images with values in one-to-one correspondence with the range data. This is a considerable simplification with respect to the use of reflectance information in order to eliminate texture's artifacts, since the reflectance has to be acquired independently of the geometry's information. The proposed technique, as shown in Section IV, is suited to the automatic modeling of cultural heritage objects, which is considered one of the most challenging applications of 3-D modeling.

In the introduction, we explained that low costs and limited technical skills are essential for the widespread practice of 3-D modeling in the cultural heritage field and in this connection automatic 3-D modeling procedure play a fundamental role. Automatic procedures may also play valuable services in many other areas: we are currently testing variations of the proposed method in the 3-D modeling of palatal calcs and of anatomical surfaces which are applications of odontostomatological and plastic surgery's interest respectively.

Automatic 3-D modeling can be improved in many aspects. The wide baseline matching problem is a central issue. Methods capable to deal with symmetric objects, to efficiently take into account structure and texture information, to be more accurate than the existing ones are currently investigated. Among the various approaches the one of [34] looks very promising. We are currently experimenting with extensions of the concept of spin-images which also include texture and not only shape information.

The acquisition of reflectance information is very important, unfortunately it is typically rather laborious as it needs texture acquisition under different controlled light conditions. Low cost image spectrophotometers have recently become available, which, in principle, may greatly simplify reflectance acquisition. It is worth assessing their actual possibilities with cultural heritage objects.

Hole-filling is a necessary postprocessing step for visually pleasing models, which should be included in an automatic modeling suite. The investigation of effective automatic methods for this task is an important research area [20].

The use of inexpensive acquisition equipment is also very important for cost containment, in this connection it would be worth exploring the practical performance in cultural heritage's applications of the acquisition methods of [58]–[64].

Since specular and dark surfaces are often encountered with cultural heritage objects the study of acquisition techniques capable to cope with these well known difficulties of optical acquisition methods [65] will have great value also in heritage's modeling.

Let us finally observe that in principle, 3-D models allow to be remotely seen in an interactive way, a possibility of growing interest in front of Internet's role in everyday life. Unfortunately photo-realistic textured 3-D models directly acquired from real objects can easily occupy tens if not hundreds of megabytes, differently than synthetic 3-D models of objects whose memory's occupancy is typically much lighter. Therefore the remote interactive visualization of photo-realistic 3-D models is not feasible with current Internet bandwidths, by the standard visualization paradigm, which performs the interactive visualization locally at the client's side, after the 3-D model is downloaded from the server. In this connection both the compression of textured 3-D models [66]–[73] and the investigation of alternate approaches turning the remote visualization 3-D models into a user-prompted image transmission problem [74]–[76], are very relevant research topics.

## ACKNOWLEDGMENT

The examples shown in this paper come from a 3-D modeling project between the Archaeological Museum of Bologna, Italy, the CINECA Consortium of Bologna, and the authors' group. The authors would like to acknowledge C. Morigi Govi, Director of the Archaeological Museum of Bologna, and A. Guidazzoli of CINECA for their assistance and guidance.

## REFERENCES

- [1] *Proc. IEEE CVPR Workshop on Application of Computer Vision in Archaeology, ACVA 2003*, [Online] Available: <http://www.lems.brown.edu/vision/conferences/ACVA03>.
- [2] G. Godin, J. A. Beraldin, J. Taylor, L. Cournoyer, M. Rioux, S. El-Hackim, R. Baribeau, F. Blais, P. Boulanger, J. Domey, and M. Picard, "Active optical 3-D imaging for heritage applications," *IEEE Comput. Graph. Applicat.*, pp. 24–36, Sept./Oct. 2002.
- [3] M. Levoy, K. Pulli, B. Curless, S. Rusinkiewicz, D. Koller, L. Pereira, M. Ginzton, S. Anderson, J. Davis, J. Ginsberg, J. Shade, and D. Fulk, "The digital Michelangelo project: 3-D scanning of large statues," in *Proc. SIGGRAPH Computer Graphics, Annu. Conf. Series*, 2000, pp. 131–144.
- [4] R. Baribeau, M. Rioux, and G. Godin, "Color reflectance modeling using a polychromatic laser range sensor," *IEEE Trans. Pattern Anal. Machine Intell.*, vol. 14, pp. 263–269, Feb. 1992.

- [5] F. Bernardini, I. Martin, and H. Rushmeier, "High-Quality Texture Synthesis From Multiple Scans," IBM Res., Tech. Rep. RC 21656(97598)1FEB2000, Feb. 2000.
- [6] H. Rushmeier and F. Bernardini, "The 3-D model acquisition pipeline," *Computer Graphics Forum*, vol. 21, no. 2, pp. 149–172, 2002.
- [7] F. Bernardini, I. Martin, J. Mittleman, H. Rushmeier, and G. Taubin, "Building a digital model of Michelangelo's Florentine Pietà," *IEEE Comput. Graph. Applicat.*, vol. 22, no. 1, pp. 59–67, Jan./Feb. 2002.
- [8] J. Y. Zheng and L. Z. Zhong, "Virtual recovery of excavated relics," *IEEE Comput. Graph. Applicat.*, vol. 19, pp. 6–11, May/June 1999.
- [9] D. Miyazaki, T. Ooishian, T. Nishikawa, R. Sagawa, K. Nishino, T. Tomomatsu, Y. Takase, and K. Ikeuchi, "The great buddha project: modeling cultural heritage through observation," in *Proc. 6th Int. Conf. Virtual Systems and MultiMedia (VSM 2000)*, Dec. 2000, pp. 138–145.
- [10] J.-A. Beraldin, F. Blais, L. Cournoyer, M. Rioux, F. Bernier, and N. Harrison, "Portable digital 3-D imaging system for remote sites," in *Proc. Int. Symp. Circuits System*, Monterey, CA, June 1998, pp. 412–418.
- [11] G. M. Cortelazzo and F. Marton, "3-D modeling for cultural heritage applications," in *Proc. 2nd Int. Congr. Science and Technology for the Safeguard of Cultural Heritage in the Mediterranean Basin*, Paris, France, July 1999, pp. 284–288.
- [12] L. Lucchese, G. Doretto, and G. M. Cortelazzo, "A frequency domain technique for 3-D view registration," *IEEE Trans. Pattern Anal. Machine Intell.*, vol. 24, pp. 1468–1484, Nov. 2002.
- [13] J. A. Beraldin, G. Guidi, S. Ciofi, and C. Atzeni, "Improvement of metric accuracy of digital 3-D models through digital photogrammetry. A case study: Donatello's Maddalena," in *Proc. 1st Int. Symp. 3-D Data Processing Visualization and Transmission (3-DPVT2002)*, Padova, Italy, 2002, pp. 758–761.
- [14] J. A. Beraldin, M. Picard, S. F. El-Hakim, G. Godin, C. Latouche, V. Valzano, and A. Bandiera, "Exploring a byzantine crypt through a high-resolution texture mapped 3-D model: combining range data and photogrammetry," in *Proc. Int. Workshop on Scanning for Cultural Heritage Recording*, Corfu, Greece, Sept. 2002.
- [15] —, "Virtualizing a byzantine crypt by combining high-resolution textures with laser scanner 3-D data," in *Proc. VSMM 2002*, Gyeongju, Korea, September 2002, pp. 3–14.
- [16] S. El-Hakim, J. A. Beraldin, and J. F. Lapointe, "Toward automatic modeling of monuments and towers," in *Proc. 1st Int. Symp. 3-D Data Processing Visualization and Transmission (3-DPVT2002)*, Padova, Italy, 2002, pp. 526–531.
- [17] G. Guidi, G. Tucci, J. A. Beraldin, S. Ciofi, D. Ostuni, F. Costantini, and S. El-Hakim, "Multiscale archaeological survey based on the integration of 3-D scanning and photogrammetry," in *Proc. Int. Workshop on Scanning for Cultural Heritage Recording*, Corfu, Greece, Sept. 2002, pp. 58–64.
- [18] B. Zevi, *Saper vedere l'architettura*. Torino, Italy: Einaudi, 1964.
- [19] R. Scopigno, P. Pingia, C. Rocchini, P. Cignoni, and C. Montani, "3-D scanning and rendering cultural heritage artifacts on a low budget," in *Proceedings European Workshop on High Performance Graphics Systems and Applications*. Bologna, Italy: Cineca, October 2000, pp. 16–17.
- [20] J. Davis, S. R. Marschner, M. Garr, and M. Levoy, "Filling holes in complex surfaces using volumetric diffusion," in *Proc. IEEE 1st Int. Symp. 3-D Data Processing Visualization and Transmission*, June 2002, pp. 428–438.
- [21] P. J. Besl and N. D. McKay, "A method for registration of 3-D shapes," *IEEE Trans. Pattern Anal. Machine Intell.*, vol. 14, pp. 239–259, Feb. 1992.
- [22] H. G. Mass, "Robust automatic surface reconstruction with structured light," in *Proc. Int. Archives of Photogrammetry and Remote Sensing XXIX*, 1992, pp. 709–713.
- [23] R. J. Valkenburg and A. M. McIvor, "Accurate 3-D measurement using a structured light system," *Image Vis. Comput.*, vol. 16, pp. 99–110, 1998.
- [24] E. Horn and N. Kiryati, "Toward optimal structured light patterns," in *Proc. Int. Conf. Recent Advances in 3-D Digital Imaging and Modeling*, Ottawa, ON, Canada, 1997, pp. 28–35.
- [25] M. Trobina, "Error Model of a Coded-Light Range Sensor," Res. Rep. ETH-Zentrum BIWI-TR-164, 1995.
- [26] A. Ashbrook, R. Fisher, C. Robertson, and N. Werghi, "Finding surface correspondence for object recognition and registration using pairwise geometric histograms," in *Proc. Eur. Conf. Computer Vision*, vol. 1407, 1998, pp. 674–786.
- [27] C. Dorai, G. Wang, A. Jain, and C. Mercer, "Registration and integration of multiple object views for 3-D model construction," *IEEE Trans. Pattern Anal. Machine Intell.*, vol. 20, pp. 83–89, Nov. 1998.
- [28] K. Higuchi, M. Hebert, and K. Ikeuchi, "Building 3-D models from unregistered range images," *Graph. Mod. Imag. Process.*, vol. 57, no. 4, pp. 315–333, 1995.
- [29] D. Huber and M. Hebert, "Fully automatic registration of multiple 3-D data sets," in *Proc. IEEE Workshop on Computer Vision Beyond the Visible Spectrum*, Dec. 2001, pp. 433–449.
- [30] D. Zhang and M. Hebert, "Harmonic maps and their applications in surface matching," in *Proc. IEEE Conf. Computer Vision and Pattern Recognition (CVPR 99)*, Nov. 1999, pp. 524–530.
- [31] A. E. Johnson, "Spin-Images: A Representation for 3-D Surface Matching," Ph.D. dissertation, Carnegie Mellon Univ., Pittsburgh, PA, Aug. 1997.
- [32] A. E. Johnson and M. Hebert, "Using spin-images for efficient multiple model recognition in cluttered 3-D scenes," *IEEE Trans. Pattern Anal. Machine Intell.*, vol. 21, no. 5, pp. 433–449, 1999.
- [33] P. Krsek, T. Pajdla, V. Hlavac, and R. Martin, "Range image registration driven by hierarchy of surface differential features," in *Proc. 22nd Workshop of the Austrian Association for Pattern Recognition*, May 1998, pp. 175–183.
- [34] J. Vanden Wyngaerd and L. Van Gool, "Coarse registration of surface patches with local symmetries," in *Proc. Eur. Conf. Computer Vision (ECCV'02)*, vol. 2351, May 2002, pp. 572–586.
- [35] J. Vanden Wyngaerd, L. Van Gool, R. Koch, and M. Proesmans, "Invariant-based registration of surface patches," in *Proc. Int. Conf. Computer Vision (ICCV'99)*, 1999, pp. 301–306.
- [36] L. Van Gool, D. Vandermeulen, G. Kalberer, T. Tuytelaars, and A. Zalesny, "Modeling shapes and textures from images: new frontiers," in *Proc. of 1st Int. Symp. 3-D Data Processing Visualization and Transmission (3-DPVT2002)* Padova, Italy, June 2002, pp. 286–294.
- [37] G. Roth, "Registering two overlapping range images," in *Proc. 2nd Int. Conf. on 3-D Digital Imaging and Modeling*, Ottawa, ON, Canada, October 1999, pp. 191–200.
- [38] B. K. P. Horn, *Computer Vision*. New York: McGraw-Hill, 1987.
- [39] Y. Chen and G. G. Medioni, "Object modeling by registration of multiple range images," *Image Vis. Comput.*, vol. 10, no. 3, pp. 145–155, 1992.
- [40] Z. Zhang, "Iterative point matching for registration of free-form curves and surfaces," *Int. J. Comput. Vis.*, vol. 13, no. 2, pp. 119–152, 1994.
- [41] T. Jost and H. Hügli, "A multi-resolution scheme ICP algorithm for fast shape registration," in *Proc. 1st Int. Symp. 3-D Data Processing Visualization and Transmission (3-DPVT2002)* Padova, Italy, 2002, pp. 540–543.
- [42] C. Kapoutsis, C. Vavoulidis, and I. Pitas, "Morphological iterative closest point algorithm," *IEEE Trans. Image Processing*, vol. 8, pp. 1644–1646, Nov. 99.
- [43] M. Greenspan and G. Godin, "A nearest neighbor method for efficient ICP," in *Proc. 3rd Int. Conf. 3-D Digital Imaging and Modeling*, Quebec City, QC, Canada, May 2001, pp. 161–168.
- [44] S. Rusinkiewicz and M. Levoy, "Efficient variants of the ICP algorithm," in *Proc. 3rd Int. Conf. 3-D Digital Imaging and Modeling*, Quebec City, QC, Canada, May 2001, pp. 145–152.
- [45] H. Hügli and C. Schültz, "Geometric Matching of 3-D objects: assessing the range of successful initial configuration," in *Proc. Int. Conf. 3-D Digital Imaging and Modeling*, Ottawa, ON, Canada, 1997, pp. 101–106.
- [46] A. Johnson and S. Kang, "Registration and integration of textured 3-D data," in *Proc. Int. Conf. Recent Advances in 3-D Digital Imaging and Modeling*, Ottawa, ON, Canada, May 1997, pp. 234–241.
- [47] R. Benjema and F. Schmitt, "Fast Global registration of 3-D sampled surfaces using a multi-z-buffer technique," in *Proc. Int. Conf. Recent Advances in 3-D Digital Imaging and Modeling*, Ottawa, ON, Canada, May 1997, pp. 113–120.
- [48] D. W. Eggert, A. W. Fitzgibbon, and R. B. Fisher, "Simultaneous registration of multiple range views for use in reverse engineering of CAD models," *Comput. Vis. Image Understand.*, vol. 69, no. 3, pp. 253–272, Nov. 1998.
- [49] K. Pulli, "Multiview registration for large data sets," in *Proc. 2nd Int. Conf. on 3-D Digital Imaging and Modeling*, Ottawa, ON, Canada, October 1999, pp. 113–120.
- [50] R. Bergevin, M. Soucy, H. Gagnon, and D. Laurendeau, "Toward a general multiview registration technique," *IEEE Trans. Pattern Anal. Machine Intell.*, vol. 18, no. 5, pp. 540–547, 1996.
- [51] K. Pulli, "Surface Reconstruction and Display from Range and Color Data," Ph.D. dissertation, Univ. Washington, Seattle, 1997.
- [52] R. Lenz, P. Meer, and M. Hauta-Kasari, "Spectral-based illumination estimation and color correction," *Color Res. Applicat.*, vol. 24, no. 2, pp. 98–111, April 1999.
- [53] A. H. Munsell, *Book of Color*. Baltimore, MA: Matte Finish Collection, 1976.

- [54] G. M. Cortelazzo and L. Lucchese, "A new method of image mosaicking and its application to cultural heritage representation," in *Comput. Graph. Forum*, vol. 18, 1999, pp. 265–275.
- [55] P. J. Burt and E. H. Adelson, "A multiresolution spline with application to image mosaics," *ACM Trans. Graph.*, vol. 2, no. 4, pp. 217–236, Oct. 1983.
- [56] C.-T. Hsu and J.-L. Wu, "Multiresolution Mosaic," in *Proc. ICIP'96*, vol. 3, Sept. 1996, pp. 743–746.
- [57] *PolyWorks User's Guide Ver. 5.0*, InnovMetric Software Inc., Sainte Foy, Canada, Jan. 2001.
- [58] R. Cipolla and P. Giblin, *Visual Motion of Curves and Surfaces*. Cambridge, U.K.: Cambridge Univ. Press, 2000.
- [59] J. Bouguet and P. Perona, "3D photography on your desk," in *Proc. 6th Int. Conf. Computer Vision*, Bombay, India, January 1998, pp. 43–50.
- [60] —, "3d photography using shadows in dual-space geometry," *International Journal of Computer Vision*, vol. 35, no. 2, pp. 129–149, November–December 1999.
- [61] S. Savarese, H. Rushmeier, F. Bernardini, and P. Perona, "Implementation of a shadow carving system for shape capture," in *Proc. of 1st International Symposium on 3-D Data Processing Visualization and Transmission (3-DPVT2002)*. Padova, Italy: IEEE Press, 2002, pp. 12–23.
- [62] C. H. Esteban and F. Schmitt, "Multi-stereo 3-D object reconstruction," in *Proc. 1st Int. Symp. 3-D Data Processing Visualization and Transmission (3-DPVT2002)*, Padova, Italy, 2002, pp. 159–166.
- [63] F. Schmitt and Y. Yemez, "3-D color object reconstruction from 2-D image sequences," in *IEEE Int. Conf. Image Processing*, Kobe, Japan, 1999.
- [64] C. Colombo, A. Del Bimbo, and F. Pernici, "Uncalibrated 3-D metric reconstruction and flattened texture acquisition from a single view of a surface of revolution," in *Proc. 1st Int. Symp. 3-D Data Processing Visualization and Transmission (3-DPVT2002)*, Padova, Italy, June 2002, pp. 277–284.
- [65] S. Savarese, M. Chen, and P. Perona, "Second order local analysis for 3-D reconstruction of specular surfaces," in *Proc. 1st Int. Symp. 3-D Data Processing Visualization and Transmission (3-DPVT2002)*, Padova, Italy, 2002, pp. 356–361.
- [66] V. Bajaj, V. Pascucci, and G. Zhuang, "Single resolution compression of arbitrary triangular meshes with properties," *Comput. Geometry: Theory Applicat.*, vol. 14, pp. 167–186, 1999.
- [67] P. Cignoni, C. Montani, and R. Scopigno, "A comparison of mesh simplification algorithms," *Comput. Graph.*, vol. 22, no. 1, pp. 37–54, 1998.
- [68] B. Kronrod and C. Gotsman, "Optimized compression of triangle mesh geometry using prediction trees," in *Proc. 1st Int. Symp. 3-D Data Processing Visualization and Transmission (3-DPVT2002)*, Padova, Italy, 2002, pp. 602–608.
- [69] The Web3-D Consortium, [Online] Available: <http://www.web3d.org/>
- [70] G. Taubin, W. Horn, F. Lazarus, and J. Rossignac, "Geometry coding and VRML," *Proc. IEEE*, vol. 86, pp. 1228–1243, June 1998.
- [71] G. Taubin and J. Rossignac, "Geometric compression through topological surgery," *ACM Trans. Graph.*, vol. 17, no. 2, pp. 84–115, 1998.
- [72] P. Cignoni, C. Montani, C. Rocchini, R. Scopigno, and M. Tarini, "Preserving attribute values on simplified meshes by re-sampling detail textures," *Vis. Comput.*, vol. 15, no. 10, pp. 519–539, 1999.
- [73] M. Isenburg and J. Snoeyink, "Coding with ASCII: compact, yet text-based 3-D content," in *Proc. 1st Int. Symp. 3-D Data Processing Visualization and Transmission (3-DPVT2002)*. Padova, Italy, 2002, pp. 609–616.
- [74] M. Levoy, "Polygon-assisted JPEG and MPEG compression of synthetic images," in *Proc. SIGGRAPH Computer Graphics Proceedings Annu. Conf. Series*, 1995, pp. 21–28.
- [75] K. Engel, O. Sommer, and T. Ertl, "A framework for interactive hardware accelerated remote 3-D-visualization," in *Proc. VisSym Joint Eurographics-IEEE TCVG Symp. Visualization*, 2000, pp. 167–177.

- [76] R. Bernardini, G. M. Cortelazzo, and G. Tormen, "IBR-based compression for remote visualization," in *Proc. 1st Int. Symp. 3-D Data Processing Visualization and Transmission (3-DPVT2002)*, Padova, Italy, June 2002, pp. 513–519.



**Marco Andreetto** was born in Este, Italy, in 1976. He received the "Laurea in Ingegneria Informatica" degree from the University of Padova, Padova, Italy, in 2001, and he is currently pursuing the Ph.D. degree at the California Institute of Technology, Pasadena.

His research interests are computer vision, computer graphics, 3-D modeling, and image processing.



**Nicola Brusco** was born in Caprino Veronese, Italy, in 1977. He received the "Laurea in Ingegneria Informatica" degree from the University of Padova, Padova, Italy, in 2002, and he is currently pursuing the Ph.D. degree in the Department of Information Engineering of the University of Padova.

He is a Research Assistant with the Multimedia Telecommunications and Technology Laboratory at the University of Padova. His research interests are 3-D models compression and transmission, computer vision, and computer graphics.



**Guido Maria Cortelazzo** was born in Este, Italy, in 1952. He received the "Laurea in Ingegneria Elettronica" degree from the University of Padova, Padova, Italy, in 1976, and the M.S. degree and Phil. Dr. degree both in electrical engineering from the University of Illinois at Urbana-Champaign, in 1980 and 1984, respectively.

From 1983 to 1986, he was with M/A-COM Linkabit, a satellite communication company of San Diego, CA. In 1986, he joined the Department of Information Engineering (DEI) of the University of Padova where he is now Full Professor. In 1986, he funded with colleague G. A. Mian the Image Processing Laboratory of DEI and, in 1993, the Multimedia Telecommunications and Technology Laboratory of DEI, which he is still directing. In 1998 he was Visiting Associate with the California Institute of Technology, Pasadena. His current research interests concern interactive scene representation both by model-based and image-based methods, the transmission and the distributed visualization of 3-D data and interactive scene representations. He is the author of more than 50 journal papers. He is currently a Guest Editor of a special issue of *Computer Vision and Image Understanding* on "model-based and image-based 3-D scene representation for interactive visualization."

Dr. Cortelazzo co-chaired the 1st International Symposium on 3-D Data Processing Visualization and Transmission.